Deuterium Magic Angle Spinning Studies of Substrates Bound to Cytochrome P450†

Hyerim Lee,‡ Paul R. Ortiz de Montellano,§ and Ann E. McDermott*,‡

Department of Chemistry, Columbia University, New York, New York 10027, and Department of Pharmaceutical Chemistry, School of Pharmacy, S-926 University of California, San Francisco, San Francisco, California 94143-0446

Received February 26, 1999; Revised Manuscript Received May 17, 1999

ABSTRACT: We report solid-state deuterium magic angle spinning NMR spectra of perdeuterated adamantane bound to the active site of microcrystalline cytochrome $P450_{cam}$ ($CP450_{cam}$) in its resting state. $CP450_{cam}$ contains a high-spin ferric (Fe^{3+}) heme in the resting state; the isotropic shift was displaced from the diamagnetic value and varied with temperature consistent with Curie-law dependence. A nondeuterated competitive tighter binding ligand, camphor, was used to displace the adamantane-bound species. This addition resulted in the disappearance of the hyperfine-shifted signal associated with a perdeuterated adamantane bound to $CP450_{cam}$, while signals presumably associated with adamantane bound to other cavities persisted. We simulated the deuterium spinning side-band intensities for the enzyme-bound species using dipolar hyperfine coupling as the only anisotropic interaction; the deuterium quadrupolar interaction was apparently averaged due to a fast high-symmetry motion. These data provide direct support for previous proposals that substrates are conformationally mobile on the time scale of enzymatic turnover. The simulations suggested that the adamantane binds with an average metal-deuterium distance of 6.2 (±0.2) Å, corresponding to a dipolar coupling constant of 6.5 (±0.5) kHz.

Cytochrome P450 (CP450)[1] enzymes catalyze the hydroxylation of an impressive range of aromatic and aliphatic substrates in the contexts of detoxification, drug metabolism, and biosynthesis. Among these enzymes, the cytochrome P450 camphor 5-exo-hydroxylase ($CP450_{cam}$) has been the most extensively studied in terms of structure and mechanism. $CP450_{cam}$ is a 45 kDa polypeptide chain containing a single ferric (Fe^{3+}) protoporphyrin IX in the resting state (*1*). It hydroxylates (1*R*)-camphor to form a dominant product, (1*R*)-5-*exo*-hydroxycamphor. The enzyme has an active site in which the heme iron (III) atom is hexacoordinate, with the sulfur atom of Cys-357 acting as one axial heme ligand and a water molecule (*2*) as the other axial ligand in the resting state (*1, 3*) (Figure 1). Upon substrate binding, the heme iron(III) becomes high spin with EPR *g* values of 8.0, 4.0, and 1.81 (g_x, g_y, and g_z) (*27*).

According to one popular mechanism (*4*) (Figure 2), the substrate binds to the active-site cavity close to the iron center but not directly ligated to the metal. Substrate binding is believed to trigger the following events: electron transfer, O_2 binding to Fe, a second reduction (1 e^-), protonation, and heterolytic cleavage of the C−H bond followed by "oxygen rebound". The resulting oxyferryl heme species is thought to deliver an oxygen atom to the substrate. There are many interesting questions that need to be answered concerning this enzyme's mechanism, including the precise nature of the oxygen activation step, and the roles of specific residues in the mechanism.

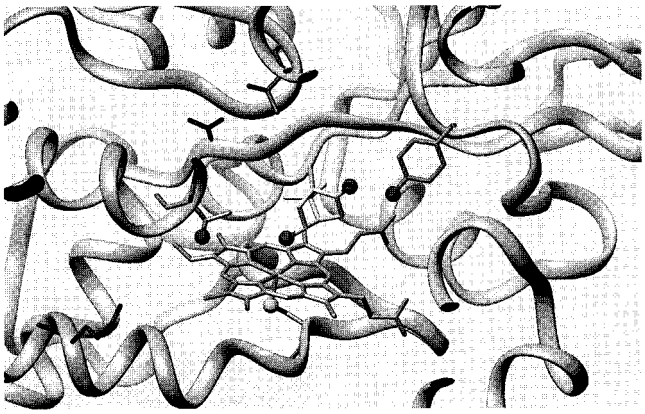

FIGURE 1: Cartoon of the complex formed by $P450_{cam}$ and its product, 5-exo-hydroxy camphor (based on the structure by T. L. Poulos and co-workers (*26*), protein databank accession code, 1noo). The proximal ligand, Cys-357 is coordinated to the iron of the heme at the active site. Tyr-96 is presumed to play an important role in catalysis by positioning the camphor substrate with a hydrogen bond. Thr-252 is proposed to participate in solvent "tunnels" and proton delivery.

Here we focus on the substrate motion of $CP450_{cam}$ and its possible relation to product control. Substrate mobility

† This work was supported by a grant to the Columbia Environmental Molecular Sciences Institute from the National Science Foundation and the Department of Energy, Grant NSF CHE 98-10367 (A.E.M.), and NIH Grants GM 49964 (A.E.M.) and GM 25515 (P.R.O.M.) and Kanagawa Academy of Science and Technology (A.E.M.). Ann McDermott is a Cottrell Scholar of Research Corporation.

* To whom correspondence should be addressed: Havemeyer Hall, Department of Chemistry, Columbia University, 3000 Broadway, New York, NY 10027. Phone: (212) 854-8393. Fax: (212) 932-1289. E-mail: mcdermot@chem.columbia.edu.

‡ Columbia University.

§ University of California. Phone: (415) 476−2903. Fax: (415) 502−4728. E-mail: ortiz@cgl.ucsf.edu.

[1] Abbreviations: MAS, magic angle spinning; SSNMR, solid-state nuclear magnetic resonance; CP450, cytochrome P450; $CP450_{cam}$, cytochrome P450 camphor 5-exo-hydroxylase; FID, free induction decay.

10.1021/bi990463l CCC: $18.00
Published on Web 07/24/1999

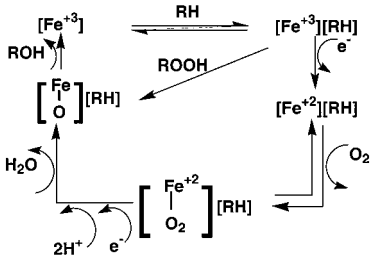

FIGURE 2: Proposed catalytic cycle of cytochrome P450. RH = substrate, ROH = product and the heme is represented by an iron in brackets (from ref *4*).

has been proposed to be responsible for the high specificity of the enzyme for the tertiary over the secondary C−H bonds; for a wide variety of substrates, the enzyme was able to choose the weaker tertiary C−H bond, rather than oxidizing the stronger secondary bond due to specific positioning of the substrate (*5*). Substrate motion has also been suggested based on kinetic analysis of the hydroxylation involving deuterium kinetic isotope effects and product ratios; it was probed by the hydroxylation of alkanes and cyclopropanes for rat liver microsomal CP450 (*6*, *7*). Furthermore, the abstraction of hydrogen from a more congested side of a substrate, followed by oxygen rebound which occurred with retention of stereochemistry, was observed by separate studies (*8*), indicating that substrate motion is slow compared to oxygen rebound. It has also been proposed that substrate motion is required for substrate positioning and catalytic function (*9*). On the other hand, a strong correlation was observed between substrate mobility and hydroxylation inefficiency and loss of hydroxylation regiospecificity (*10*). Thus, substrate mobility has been proposed and connected to catalysis in many respects.

Many studies of isotope effects in CP450 chemistry support the model that substrates are mobile on the time scale of turnover. This is an unusual application of isotope effects in biochemistry and deserves some comment. The rate-determining step for the CP450 catalytic cycle is believed to be the electron transfer and subsequent irreversible generation of the reactive oxene−heme complex (on the left of Figure 2). Typically, one would not expect to observe deuterium isotope effects associated with steps that are not rate determining. In the case of CP450 chemistry, however, competition between alternate pathways for this reactive intermediate, for example, branching to other positions due to substrate motion or reaction with water, influence the products and can result in apparent negative or positive isotope effects. This has been extensively discussed in the literature, including a succinct review (*11*). The reactive enzyme intermediate can apparently select between several sites of differing isotopic composition, and therefore the isotope effect is "unmasked". One might consider a hypothesis that the enzyme binds the substrate in several conformations, all of which are essentially static on the enzyme. Many of the reported isotope effects, however, cannot be explained in this way. For instance, many of the experiments involve otherwise symmetric compounds that are isotopically substituted in one of two equivalent sites, and isotope effects as large as 10 are observed. The hypothesis that such a strong selection between a deuterated or protonated site occurs during binding is not likely. It would appear that the enzyme is able to actively select between the two pseudoequivalent sites during the time scale of chemical attack or during the lifetime of the reactive oxene−heme complex. Furthermore, systematic trends in the isotope effects with respect to steric bulk support the hypothesis that product branching associated with extensive and rapid substrate motion is the major reason for apparent isotope effects in the case of smaller substrates. Thus, the anomalous isotope effects seen in cytochrome P450 have often been utilized as probes of substrate motion and/or uncoupled chemistry. For example, Jones et al. have argued that the magnitude of the intramolecular isotope effect, which is observed in the oxidation of two equivalent groups in a substrate that only differ in that one is deuterated and the other is not, is highly dependent on the rate at which the positions of the two groups exchange positions within the active site (*12*−*14*). Thus, the observed kinetic isotope effects for the hydroxylation of an undeuterated versus a deuterated methyl group in *o*-xylene, *p*-xylene, and 4,4′-dimethylbiphenyl, in which the distances between the methyls are 2.48, 6.62, and 11.05 Å, respectively, were found to be 10.6 ± 0.41, 7.4 ± 0.37, and 2.7 ± 0.11. A molecular dynamic analysis of the predicted oxidation of these substrates by cytochrome $P450_{cam}$ has provided theoretical support for the postulated relationship between distance and the isotope effect (*15*). The degree of mobility is presumably substrate dependent. Whereas the methyl groups of *o*-xylene were found to exchage 1172 times in 500 ps of molecular dynamics simulations, the corresponding number of exchanges for *m*-xylene, *p*-xylene, and 4,4′-dimethylbiphenyl were found to be 77, 3, and 0. Kinetic isotope effects experiments have also been used to support the view that substrate motion within the active site of mammalian cytochrome P450 enzymes occurs readily (*16*−*20*).

In summary, many laboratories have observed anomalous isotope effects apparently associated with substrate mobility on the time scale of turnover, and these studies have been supported by computational work. Kinetic isotope effects, product ratios, and the molecular dynamics studies provide indirect evidence that the substrate is highly mobile within the active site of cytochrome $P450_{cam}$ (*15*). These studies have implied that substrate motion is fast relative to reaction rate of the intermediate iron-oxo species, but that motion of the carbon-centered radical derived from the substrate is slow relative to the rate of oxygen rebound (*6*). Our experiments are aimed at directly probing this putative substrate motion to further elucidate the origin of these isotope effects and to help rationalize the products of this enzyme.

Despite the fact that paramagnetic systems can be challenging to study by NMR, solid-state ^2H NMR has proven its advantages in several studies of motion (*21*) and structure of paramagnetic systems including small complexes (*22*) and biological systems (*23*). Thus, solid-state deuterium NMR has been shown to be a useful technique for detecting the signals in ligands coordinated to transition metals. Detection of deuterium signals from sites quite close to the metal is possible for a variety of paramagnetic species (*22*). Solid-state deuterium NMR allows elucidation of structure around the metal, characterization of the electron spin states, and the use of probes of the conformational dynamics of the molecule. For these studies, one needs to incorporate deuterium at the specific site of interest. Deuterium MAS spectra exhibit a large number of spinning side bands whose intensity pattern gives information about motion of the

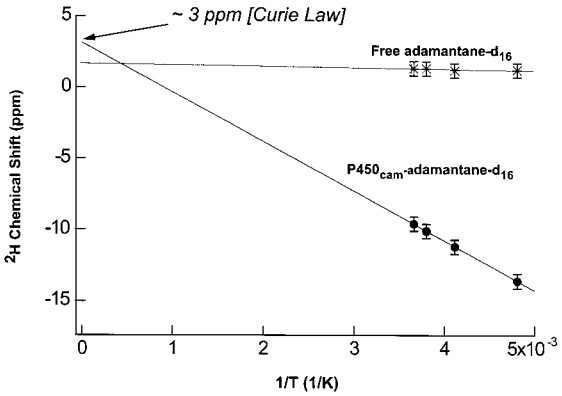

FIGURE 3: Deuterium chemical shifts of the center peak are plotted against the inverse of the absolute temperatures. The centerband positions for the solid-state MAS signal were determined from the linear fit of spinning side-band frequencies. The deuterium chemical shift of the adamantane-d_{16} bound species shows Curie behavior. The shift of the free adamantane-d_{16} species and solvent are invariant over temperature, indicating a diamagnetic environment.

deuterons of interest and the strength of the interactions. Deuterium line-shape analysis is needed to reveal characteristics of the motion. For instance, reduced intensity of the outer side bands and increased intensity of the inner side bands unambiguously indicate fast limit motion. We recently simulated the deuterium line shape for deuterated ligands in many small paramagnetic complexes (*24*). Here we present deuterium line shape analysis of perdeuterated adamantane bound to $CP450_{cam}$. This result not only verifies that the substrate motion is mobile when bound at the active site, but also provides information on the metal-substrate distance.

MATERIALS AND METHODS

Materials. Adamantane-d_{16} was purchased from Cambridge Isotope Lab. and camphor was obtained from Aldrich.

$CP450_{cam}$/Adamantane-d_{16} Complex. $CP450_{cam}$ was initially purified as the camphor-bound enzyme−substrate complex, and substrate-free $CP450_{cam}$ (camphor-free) was prepared by dialysis. A 61 μM $CP450_{cam}$ solution was dialyzed overnight at 4 °C against 50 mM NaPi, pH 7.0, followed by a second dialysis using 50 mM KPi, pH 7.0, containing 250 mM KCl. To reduce the background NMR signals from natural abundance deuterium, deuterium-depleted water purchased (Cambridge Isotope Lab.) was used in making the buffers. Adamantane-d_{16} (in 0.3 mL of ethanol) was added to 30 mL of camphor-free $P450_{cam}$ solution, resulting in its final concentration which was 50 times greater than that of $CP450_{cam}$. The ethanol volume did not exceed 1% of the final solution. The solution was incubated at 4 °C with gentle stirring overnight. The NMR sample was precipitated using 43% (w/v final) ammonium sulfate.

UV−Vis Spectral Analysis. The camphor-free $P450_{cam}$ solution had a maximum absorbance at 417 nm, while the $P450_{cam}$/adamantane-d_{16} complex showed a maximum absorbance at 390 nm. After displacing adamantane-d_{16} from $CP450_{cam}$ with nonlabeled camphor, the sample was characterized by UV−vis to confirm that $P450_{cam}$ was in a complex form with the camphor. The sample showed a maximum absorbance at 390 nm as expected.

Solid-State NMR Experiments. NMR spectra were recorded on a Chemagnetics 400 CMX spectrometer with a Larmor frequency of 60.86 MHz for deuterium. Spectra were collected using the Bloch decay sequence with a 0.1 s recycle delay. The 90° pulse length was 4.5 μs and the dwell time was 2 μs. Each spectrum was accumulated for 1−2 h corresponding to $\sim 8 \times 10^4$ scans. The amount of protein used for NMR experiments was 20−30 mg (0.4−0.7 μmol). We subsequently introduced nonlabeled camphor (8 μmol, 12−18 times excess over protein) to displace the bound adamantane-d_{16}, in order to confirm the origin of the solid-state deuterium signal. This displacement was conducted directly in the NMR sample rotor which contained the $CP450_{cam}$-adamantane-d_{16} complex.

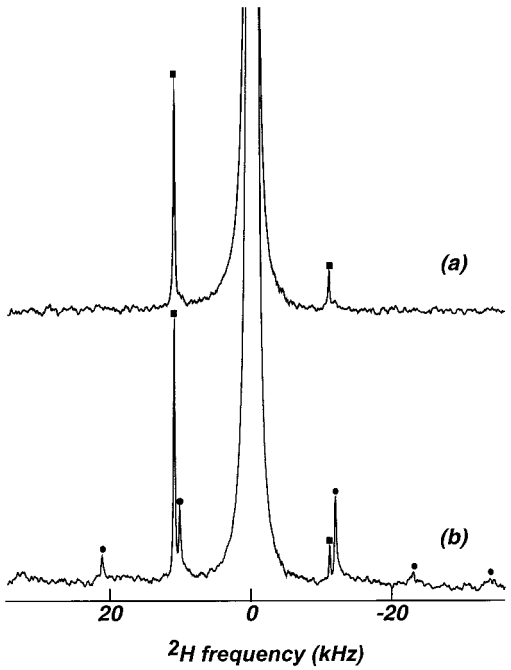

FIGURE 4: Deuterium solid-state MAS NMR spectra of (a) adamantane-d_{16} free species after displacing adamantane-d_{16} at the active site with nonlabeled camphor (b) adamantane-d_{16} bound to high-spin iron(III) at the active site of $CP450_{cam}$. The K_d values of adamantane and camphor are 50 and 3 μM, respectively. The signal due to adamantane-d_{16} is marked with circles and the signal of free adamantane is marked with squares. Both spectra were taken at 0 °C; the sample was spun at 9 kHz. The truncated free induction decay starts at the first rotor echo at 44 μs; 200 Hz line broadening was applied. The center bands of the deuterium signal were buried under the broad baseline of the free adamantane-d_{16} and a solvent peak.

Data Processing. We deleted initial data points so that the free induction decay started at the top of the first rotor echo, to prevent phase distortions. We applied 200 Hz line broadening before the Fourier transformation. The center band of the solid-state MAS deuterium NMR signal was buried under the broad baseline of the free adamantane-d_{16} and a solvent peak in solution. We confirmed the isotropic shifts based on the center band position, which was extrapolated from a linear fit of the spinning side band positions from the spectra taken using different spinning speeds.

RESULTS AND DISCUSSION

We have observed a deuterium solid-state NMR signal which we assigned to the adamantane-d_{16} bound at the active site of $CP450_{cam}$ as elaborated below. Another deuterium signal with a center band at around 1.2−1.3 ppm was assigned to adamantane-d_{16} either off the enzyme or bound

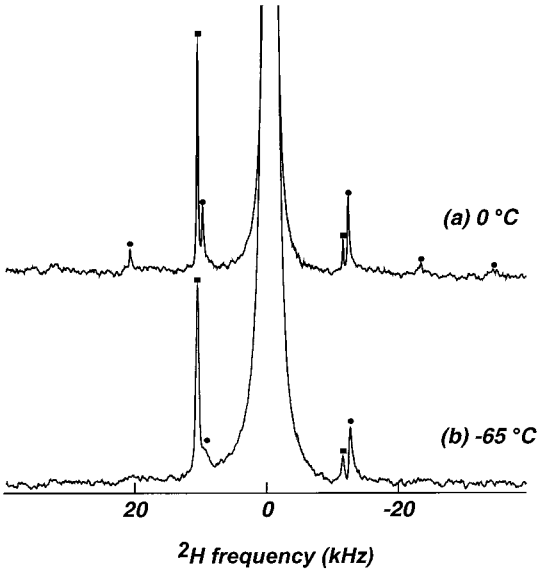

FIGURE 5: Deuterium solid-state MAS NMR spectra of adamantane-d_{16} bound to high-spin iron (III) at the active site of CP450cam. The spectra were acquired at (a) 0 °C and (b) −65 °C. The signal of the adamantane-d_{16} bound species is marked with circles, and the signal of the free species with squares. A total of 7.68×10^4 scans were added up to form the final spectra. The sample was spun at 9 kHz. The truncated free induction decay starts at the first rotor echo at 44 μs; 200 Hz line broadening was applied. The dramatic broadening of the adamantane signal at −65 °C probably indicates the onset of intermediate-exchange conformational dynamics for adamantane at the active site. The center bands of the deuterium signal were buried under the broad baseline of the free adamantane-d_{16} and a solvent peak.

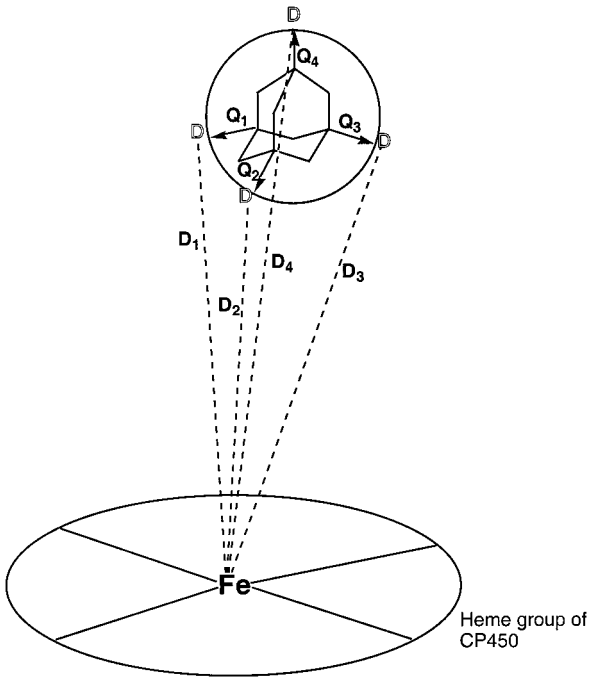

FIGURE 6: A simplified cartoon describing two tensor interactions of adamantane while bound to iron (III) center at the active site of CP450$_{cam}$. Tetrahedral symmetry-related sites in adamantane are shown as four deuterons. A quadrupolar tensor for each deuteron is denoted as Q_i, and a dipolar tensor as D_i, where i = 1, 2, 3, or 4. Two tensor interactions for each site were computed by rotating the dipolar tensor into the axis system of the quadrupolar tensor at each of the four sites. Subsequently, the four tensors were averaged. Due to the high symmetry relating the four sites, the quadrupolar tensors averaged to zero under fast motion, but not the dipolar tensors. The dipolar tensors are in a low symmetry environment, which result in a nonzero spatial average.

to another enzyme pocket distant from the paramagnetic center. Since the center band of the bound signal was buried under the broad base of the adamantane-d_{16} free signal and a solvent peak, we calculated the isotropic chemical shift using the spinning side bands from NMR spectra collected with different spinning speeds of 7 and 9 kHz. The isotropic chemical shifts were −9.6, −10.1, −11.2, and −13.6 ppm (±0.5 ppm) at 0, −10, −30, and −65 °C (respectively) with line widths of 4−7 ppm. Thus, the deuterium signal associated with the bound state species showed a strong temperature dependence of the isotropic shift, following Curie-law behavior, as expected for a paramagnetic system. On the other hand, the chemical shift of the free signal was invariant over the temperature range (Figure 3). The infinite temperature's intercept of a linear fit of shifts against inverse temperatures for the bound species, 3.15 ± 0.5 ppm, indicated that the paramagnetic shift approaches the diamagnetic region at infinite temperature as expected for a simple Curie behavior. We collected the NMR spectrum of the adamantane-d_{16} free ligand and identified its isotropic shift to be at 1.3 ppm.

We subsequently introduced a 15-fold excess of nondeuterated camphor to the same NMR sample as a competitive ligand. Since the K_d value of camphor is 3 μM, as compared with 50 μM for adamantane (*5*), we would expect camphor to displace the adamantane. As expected, camphor addition resulted in the disappearance of the paramagnetically shifted signals, but the peak in the diamagnetic region remained (Figure 4). Thus, we demonstrated that the peak at −9.6 ppm at 0 °C is due to the deuterated adamantane bound at the active site of CP450$_{cam}$. We measured the approximate T_1 values for both signals in the enzyme sample; they were 20 and 40 ms for bound adamantane-d_{16} and free adamantane-d_{16}, respectively.

The side-band intensity pattern for the deuterium signal of the adamantane-d_{16} bound species was analyzed for the temperatures 0 and −30 °C to determine the effective quadrupolar coupling constant and the dipolar hyperfine strength. At −65 °C, the peak became much broader and the spinning side bands at the outer region of the spectrum disappeared (Figure 5), so this spectrum could not be analyzed. This is due to either onset of intermediate exchange or paramagnetic broadening. The intensity pattern of spinning side bands for the bound species was asymmetric, which is the characteristic of paramagnetic compounds. Even without simulation, it is clear that the narrow pattern in the intensity of the spinning side bands clearly indicates extensive motion of the substrate while bound to CP450$_{cam}$. Spinning sideband intensities for deuterium MAS spectra of paramagnetic species are simulated in general using two interactions, a deuterium quadrupolar and a hyperfine dipolar coupling interaction; the relative tensor orientations (the angle between the C−D bond axis and the metal-deuterium bond vector)

[2] $\omega_D = (\mu_0/4\pi)\mu_{eff}\gamma_D(2\pi)^{-1}r^{-3}$, where $\mu_{eff} = \beta_e^2 S(S+1)g^2H/(3k_bT)$; $g = 2$; r = the distance from the metal to deuteron, 10^{-10} m; S = spin state ($S = {}^1/_2$, $S = 1$, $S = {}^5/_2$, etc.); $H = 9.35T$; $T = 273$ *K* (0 °C); $\beta_e = 9.27 \times 10^{-24}$ J T^{-1}; $k_b = 1.38 \times 10^{-23}$ J K^{-1}; $\mu_0 = 4\pi \times 10^{-7}$ kg^{-2} A^{-2}; $\gamma_D = 2.675 \times 10^8(60/400)$ rad^{-1} T^{-1}; $\gamma_P = 2.67 \times 10^8$ rad^{-1} T^{-1}; $h = 6.626 \times 10^{-34}$ J s.

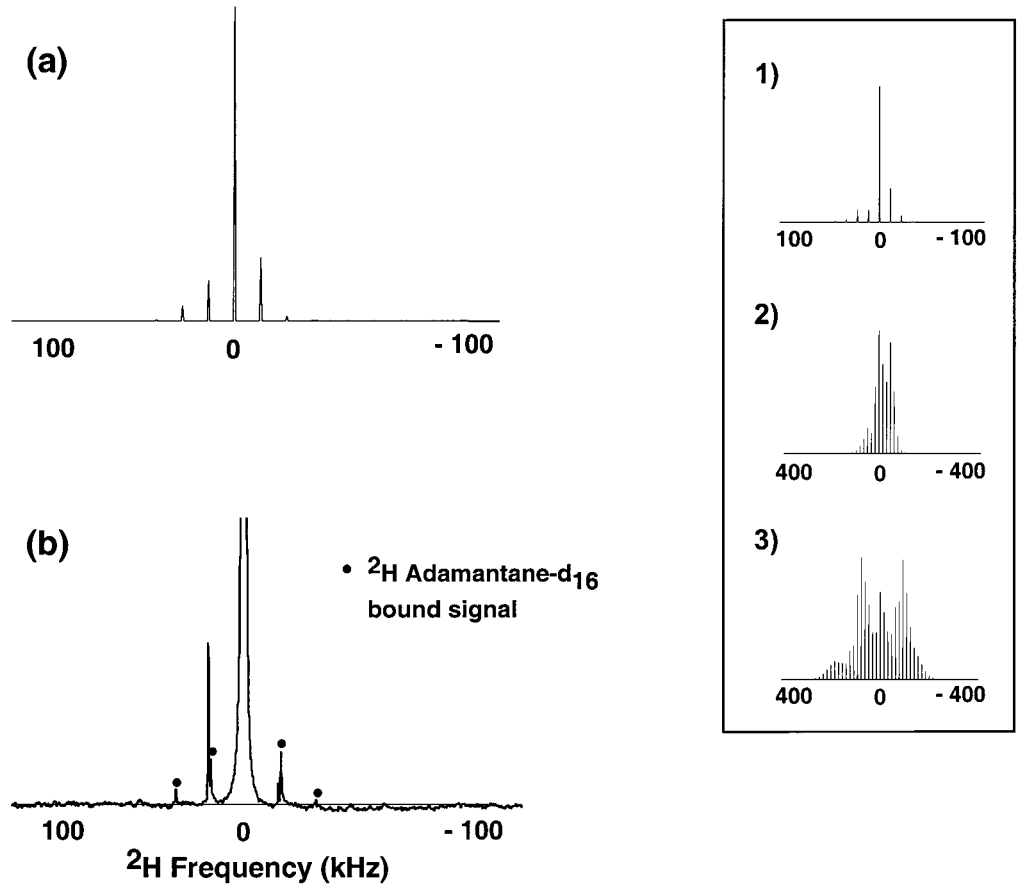

FIGURE 7: ^{2}H MAS NMR spectra of perdeuterated adamantane bound to CP450$_{cam}$. (a) A spectrum simulated using a dipolar coupling constant of 6−7 kHz assuming no quadrupolar interaction (zero effective average) and high spin iron (III) ($S = 5/2$). The spinning side-band intensities of the experimental ^{2}H NMR spectrum can be simulated using the dipolar coupling constant of 6.5 ± 0.5 kHz, suggesting that adamantane binds to high spin iron (III) with an averaged metal-deuterium distance of 6.2 (±0.2) Å. Due in part to the high molecular symmetry (T_d), all the deuterons averaged to a single isotropic NMR shift as shown in ^{2}H MAS NMR. (b) Experimental MAS spectrum. Adamantane-d_{16} bound to high-spin iron (III) at the active site of CP450$_{cam}$. The inset demonstrates that the spinning side-band intensity pattern is sensitive to variation of a quadrupolar coupling constant. The spectra in the inset were simulated using a dipolar coupling constant of 6.5 kHz and a polar angle between two interactions of 0°, and the following quadrupolar coupling constant: (1) 7 kHz, (2) 61 kHz (a three-site hop motion, a fast limit motion regime), and (3) 167 kHz (a static limit motion regime).

are also determined in these simulations, as explained in our recent manuscript (*24*). The dipolar coupling constants were calculated as follows[2] and described as well in the manuscript (*24*). Simulation of the spinning side-band intensities for the enzyme-bound perdeuterated adamantane species was possible under the assumption of fast high-symmetry motion (T_d), but we could not simulate the data assuming a rigid substrate. As shown in Figure 6, tensorial descriptions for both the dipolar and the quadrupolar are averaged over tetrahedral symmetry-related sites in adamantane; all four sites must be represented in matrix form in any fixed frame of reference, and then a simple arithmetic average is performed (*25*). This rapid symmetric motion would result in effective disappearance of the quadrupolar interaction but not of the dipolar. The principal axis for the quadrupolar interaction assumes tetrahedrally related orientations as the molecule rotates to its four orientations; the tensor has a spatial average of zero over these four orientations. The dipolar hyperfine on the other hand is rotated to 4 very similar orientations and has a non-zero spatial average. Thus, in our simulations for a mobile substrate, no quadrupolar coupling was included, consistent with the assumption of a fast ($>10^7$ s^{-1}) high-symmetry motion. Simulations using a dipolar coupling constant between 6 and 7 kHz achieved good agreement with the intensities from the spectrum measured at 0 °C (Figure 7); RMS deviations over four spinning side bands were approximately 6%, whereas if a coupling constant of 5 or 8 kHz were used, the RMS deviation was approximately 20%. This suggests that the adamantane binds to the active site with an average metal-deuterium distance of 6.2 ± 0.2 Å. The data measured at lower temperatures (−30 °C) indicated somewhat stronger dipolar coupling constants (7−8 kHz), but these differences are close to our error limit. We also compared the average distance obtained from the simulation with the one taken from the crystal structure of CP450$_{cam}$/adamantane complex by T.L. Poulos and coworkers (*10*) (protein databank accession code 3CP4). A motionally averaged distance of 6.01 Å was obtained based on the X-ray coordinates. Therefore, we demonstrated the good agreement between the calulated average distance from the experimental spectra and the measured distance from the crystal structure. The nonspecifically bound adamantane also gave rise to very weak spinning side bands; they are exaggerated in our presentation of the spectra, because the centerband is far off scale. The intensities of these spinning side bands closely matched those for solid (pure) adamantane and cannot be fit to either quadrupolar or dipolar hyperfine interactions.

We presume that this pattern arises from the chemical shift anisotropy (and perhaps has contributions from diamagnetic susceptibility and shimming effects); such effects on the bound state species will be negligible in comparison with the noise level and so will not be discussed further.

We observed that adamantane-d_{16} showed only a single peak in the ^{2}H NMR spectrum, despite the fact that it has two distinct symmetry-related types of deuterons (methine and methylene). The spectrum of adamantane-d_{16} (free compound) was also simulated by the method described above and also exhibited a single peak, as seen in the experimental spectrum. Adamantane possesses a tetrahedral symmetry, and therefore, all deuterons are expected to be averaged out to exhibit either two chemical shifts or a single isotropic chemical shift if rapid ($>10^7$ s^{-1}) hopping of the molecule between symmetry-related sites occurs. Evidently, rapid high-symmetry (spherical) motion occurs both for the active-site bound form and for the form bound to lower affinity cavities. Camphor would be another good candidate for studies of the substrate dynamics in relation to product distribution during CP450$_{cam}$ catalysis, because it is apparently anchored by the ketone group's H-bond to the active-site tyrosine and therefore might be less mobile than adamantane.

In summary, we have measured a solid-state deuterium NMR signal of perdeuterated adamantane bound in CP450cam and have simulated the observed line shape. On the basis of previous work with characterized coordination compounds, our line-shape analysis provides metal-deuterium distances accurate to within ±0.5 Å. Here, for the first time, we extended our application of the method to a biological system, CP450$_{cam}$, to understand substrate binding and dynamics. We conclude that the average deuterium−metal distance is 6.2 Å; these data also provide the first direct evidence that (at least one) substrate undergoes rapid motion within the P450$_{cam}$ active site, as required to rationalize the observed kinetic isotope effects. This line-shape fitting method is expected to be a very useful tool for other metalloenzymes.

ACKNOWLEDGMENT

The authors thank Dr. Zhoupeng Zhang for his advice on preparing the CP450$_{cam}$ sample for NMR experiments, and Dr. Tatyana Polenova for her help with the simulation program and preparation of figures and for useful discussion.

REFERENCES

1. Poulos, T. L., Finzel, B. C., and Howard, A. J. (1986) *Biochemistry 25*, 5314−5322.
2. Goldfarb, D., Thomann, H., and Ullrich, V. (1996) *J. Am. Chem. Soc. 118*, 2686−2693.
3. Poulos, T. L., Finzel, B. C., Gunsalus, I. C., Wagner, G. C., and Kraut, J. (1985) *J. Biol. Chem. 260*, 16122−16130.
4. Ortiz de Montellano, P. R. (1995) *Cytochrome P450: Structure, Mechanism, and Biochemistry*, 2nd ed., Plenum Press, New York.
5. White, R. E., McCarthy, M.-B., Egeberg, K. D., and Sligar, S. G. (1984) *Arch. Biochem. Biophys. 228*, 493−502.
6. Atkinson, J. K., and Ingold, K. U. (1993) *Biochemistry 32*, 9209−9214.
7. Atkinson, J. K., Hollenberg, P. F., Ingold, K. U., Johnson, C. C., Le Tadic, M.-H., Newcomb, M., and Putt, D. A. (1994) *Biochemistry 33*, 10630−10637.
8. Ortiz de Montellano, P. R., and Stearns, R. A. (1987) *J. Am. Chem. Soc. 109*, 3415−3420.
9. De Voss, J. J., Sibbesen, O., Zhang, Z., and Ortiz de Montellano, P. R. (1997) *J. Am. Chem. Soc. 119*, 5489−5498.
10. Raag, R., and Poulos, T. L. (1991) *Biochemistry 30*, 2674−2684.
11. Korzekwa, K. R., Gillette, J. R., and Trager, W. F. (1995) *Drug Metab. Rev. 27*, 45−59.
12. Jones, J. P., Korzekwa, K. R., Rettie, A. E., and Trager, W. F. (1986) *J. Am. Chem. Soc. 108*, 7074−7078.
13. Jones, J. P., and Trager, W. F. (1987) *J. Am. Chem. Soc. 109*, 2171−2173.
14. Jones, J. P., Korzekwa, K. R., Rettie, A., and Trager, W. F. (1988) *J. Am. Chem. Soc. 110*, 2018.
15. Audergon, C., Iyer, K. R., Jones, J. P., Darbyshire, J. F., and Trager, W. F. (1999) *J. Am. Chem. Soc. 121*, 41−47.
16. Ichinose, R., and Kurihara, N. (1987) *Biochem. Pharmacol. 36*, 3751−3756.
17. Ebner, T., Meese, C., and Eichelbaum, M. (1995) *Mol. Pharmacol. 48*, 1978−1086.
18. Harada, N., Miwa, G., Walsh, J., and Lu, A. (1984) *J. Biol. Chem. 259*, 3005−3010.
19. Hanzlik, R. P., and Ling, K.-H. J. (1990) *J. Org. Chem. 55*, 3992−3997.
20. Hanzlik, R. P., and Ling, K.-H. J. (1993) *J. Am. Chem. Soc. 115*, 9363−9370.
21. Lin, T.-H., DiNatale, J. A., and Vold, R. R. (1994) *J. Am. Chem. Soc. 116*, 2133−2134.
22. Liu, K., Ryan, D., Nakanishi, K., and McDermott, A. (1995) *J. Am. Chem. Soc. 117*, 6897−6906.
23. Liu, K., Williams, J., Lee, H., Fitzgerald, M. M., Jensen, G. M., Goodin, D. B., and McDermott, A. E. (1998) *J. Am. Chem. Soc. 120*, 10199−10202.
24. Lee, H., Polenova, T., Beer, R., and McDermott, A. E. (1999) *J. Am. Chem. Soc.* (in press).
25. Wittebort, R. J., Olejniczak, E. T., and Griffin, R. G. (1987) *J. Chem. Phys. 86*, 5411−5420.
26. Li, H., Narashimulu, S., Havran, L. M., Winkler, J. D., and Poulos, T. L. (1995) *J. Am. Chem. Soc. 117*, 6297−6299.
27. Dawson, J. H. (1988) *Science 240*, 433−439.

BI990463L